Research of surface-enhanced Raman scattering on Ag@PMBA@C@Au hybrid nanoparticles*

TAN Enzhong** and LÜ Suye**

Liberal Study College, Beijing Institute of Petrochemical Technology, Beijing 102617, China

(Received 22 May 2023; Revised 1 September 2023)

©Tianjin University of Technology 2024

Monodispersed, biocompatible, and readily-functionalized hybrid reporter-embedded core-shell nanopartilces (NPs) have been prepared in a simple route. This composite offers a potential platform for immunochemical detection using surface-enhanced Raman scattering (SERS) due to their high sensitivity, good stability and biocompatiblity. This also provides a new platform for insight into SERS enhancement mechanism.

Document code: A **Article ID:** 1673-1905(2024)02-0065-5

DOI https://doi.org/10.1007/s11801-024-3094-5

Surface-enhanced Raman scattering (SERS) has been proved to be a powerful spectroscopic technique due to its high sensitivity in detecting and providing fingerprint information of various analyte down to single-molecule level[1-7]. Thus, preparation of SERS tagging materials has gained intense interest in biology for the investigation of the complex interplay of biomolecules. In recent years, SERS-based nanopartilces (NPs) have been synthesized as a new class of labels[8-13]. Compared to the commonly used labels, such as quantum dots and fluorescence labels, SERS labels have unique advantages, such as high sensitivity, good stability, the absence of photobleaching and the multiplex detection capability due to the fingerprint spectra of labeling molecules[14,15]. However, the as-reported SERS labels based on individual silver nanoparticle (AgNP) and gold nanoparticle (AuNP) produce relatively weak signals due to the poor enhancement ability of the individual metal NP. Theoretical and experimental results show that two mechanisms contribute to the enhancement of Raman signals, the electromagnetic (EM) mechanism[16-19] and the chemical mechanism[20-22]. The EM enhancement is the dominating contributor, especially in the gap region between the noble metal nanostructures where an extraordinary enhancement can be obtained due to the strong coupling of the EM field as so-called hot spot phenomenon. However, these hot spot nanostructures, mostly dimer or colloidal aggregation of AgNPs or AuNPs, are formed by salt-induced assembly with particles of various sizes together with different interparticle spacing[23,24]. Although great efforts have been devoted to investigate the hot spot phenomenon, the preparation of nanostructures rich in hot spots could hardly be controlled via simple chemical synthesis methods. This fact has been a main obstacle for the using of hot spot toward more advanced applications. Thus, it is a challenging and significant work to develop an easy route for fabrication of NP-based SERS labels with uniform size and strong Raman signal by residing the reporter molecules inside hot spots.

Based on the idea that controlling the nano gap between two noble metal NPs is the key to obtain reliable SERS labels with intense signals, we have developed a simple method for synthesis of reporter-embedded core-shell NP full of hot spots. Herein, AgNP was used as optical enhancement substrate, p-mercaptobenzoic acid (PMBA) was the SERS reporter molecule, carbon (C) shell was for protection of PMBA and spacing of inner AgNP and outer AuNPs. Outer AuNPs bring in hot spots due to EM field coupling with the inner AgNP. In addition, AuNPs could be further functionalized to meet the requirements of the applications in biological detection (the core-shell nanostructures are denoted as Ag@PMBA@C@Au).

Hydrogen tetrachloroaurate (III) tetrahydrate ($HAuCl_4 \cdot 4H_2O$) was purchased from Kermel Chemical Reagent Co., Ltd. (Tianjin, China). Trisodium citrate, sodium borohydride ($NaBH_4$), silver nitrate ($AgNO_3$), and glucose were bought from Beijing Chemical Reagent Company (Beijing, China). PMBA was obtained from J&K Chemical Company (Beijing, China). All reagents were used as received without further purification. All glassware was cleaned with freshly prepared aqua regia and thoroughly rinsed with deioned (DI) water prior to use.

Raman spectra were collected on a JY HR800 Raman spectrometer (France) with a He-Ne laser of 632.8 nm for excitation with a power of approximately 2 mW,

* This work has been supported by the Scientific Research Project of Beijing Educational Committee (No.KM202010017010).
** E-mail: tanenzhong@bipt.edu.cn

10× objective and 600 lines/mm gratings. Transmission electron microscopy (TEM) and high-resolution TEM (HRTEM) images were received from a JEOL JEM-2100F transmission electron microscope. UV-vis spectra were obtained on a GBC Cintra 10e spectrometer.

AgNPs with diameters of 50—70 nm were synthesized by reduction of silver nitrate using trisodium citrate according to Lee's method. Briefly, 18 mg of $AgNO_3$ was added to 100 mL of DI water and then heated to boiling. Next, 2 mL of 1% trisodium citrate solution was added dropwise with stirring. The mixture was boiling for another 15 min and then cooled down to room temperature. Whereafter, the Raman reporter molecule, PMBA, was self-assembled on the surface of AgNPs. 10 μL of PMBA ethanolic solution (1 mM) was added to 10 mL of AgNPs suspension, and then the mixture was shaken for 10 min and then stored in dark for reaction. 10 h later, the mixture was centrifuged, and then the precipitation was washed with DI water several times to remove the free PMBA. Finally, the resulting PMBA-modified AgNPs were redispersed in DI water.

In a typical experiment, 1 mL of as-prepared AgNPs suspension was added to 20 mL of glucose solution (0.5 M). After several minutes of stirring, the mixture turn clear and then was put into a 25 mL Teflon-sealed autoclave and maintained at 160 ℃ for 4 h. The resulting products were rinsed with DI water by centrifugation and then redispersed in DI water.

Different volumes (25 μL, 75 μL, 200 μL) of $HAuCl_4$ solutions (10 mM) were added to 5 mL of the above prepared colloid suspension with stirring, respectively. Next, different volumes (25 μL, 75 μL, 200 μL) of the mixed solutions of sodium citrate (20 mM) and $NaBH_4$ (50 mM) were added, respectively. Then the mixture was heated to boiling with stirring. In 15 min, the resultant was allowed to cool down to room temperature. The resulting products were stored in the refrigerator for further measurement.

Fig.1 depicts the preparation process of the hybrid NPs SERS labels. First, AgNPs with diameters of 50—70 nm were obtained by reducing $AgNO_3$ using sodium citrate. Then, the Raman reporter molecules, PMBA, were adsorbed on the surface of AgNP by Ag-S bonding. Next, labeled-AgNPs were encapsulated with a C shell through catalyzed dehydration of glucose under hydrothermal condition[25-27]. Finally, a submonolayer of AuNPs were adsorbed on the C layer surface by reducing $HAuCl_4$ using sodium citrate and $NaBH_4$. The color of the sample changed distinctly after the growth of AuNPs, which was proved by the UV-vis adsorption spectra.

The as-prepared hybrid NPs in different geometrical morphologies were characterized by UV-vis adsorption spectroscopy and TEM. Fig.2 shows the representative TEM micrographs of Ag@PMBA@C and Ag@PMBA@C@Au NPs with different Au-Ag molar ratios. From Fig.2(a) we know that the thickness of C shell is about 3—4 nm, which is an ideal distance for hot spots originating from EM coupling[18,19,28]. The representative TEM images clearly demonstrate the evolvement of morphologies of Ag@PMBA@C@Au NPs with the increase of Au to Ag molar ratios (Fig.2(b)—(d)). From TEM images, the core AgNPs in hybrid NPs (Fig.2) have similar diameters, which are about 70 nm. The Ag@PMBA@C NPs were modified by AuNPs and the density of AuNPs increased with the increase of the amount of $HAuCl_4$. In addition, the diameter of these AuNPs could be determined in range from 5 nm to 10 nm. To demonstrate elemental composition of the composite, we analyzed the Ag@PMBA@C@Au NPs with Au to Ag molar ratio at 0.40: 1.0 in TEM by the energy dispersive X-ray spectroscopy (EDX) in the TEM. From the spectrum, we known that Au and Ag were contained in the composite. And the molar ratio of Au to Ag is as high as 0.536: 0.464. Compared to the amount used in synthesis, the ratio of Au in EDX turned more. This fact may be regarded as the result of the adsorbed AuNPs distributing on the outer surface of the composite.

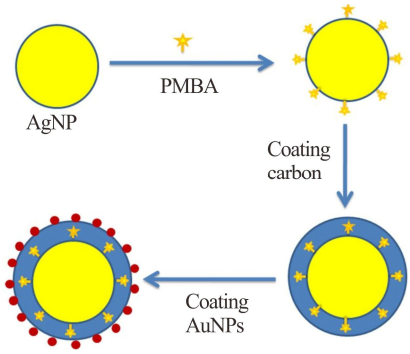


Fig.1 Schematic illustration of the preparation of Ag@PMBA@C@Au NPs by multiple steps

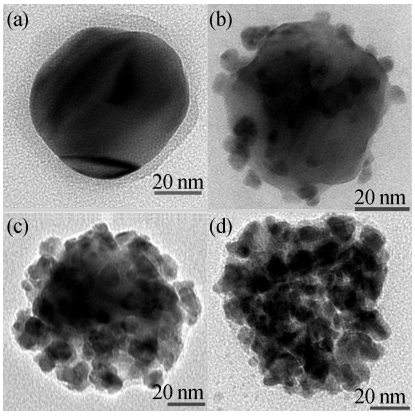


Fig.2 TEM images of core-shell NPs with different Au to Ag molar ratios: (a) 0: 1.0 (Ag@PMBA@C NPs); (b) 0.05: 1.0; (c) 0.15: 1.0; (d) 0.40: 1.0

To get more information about the hybrid NPs in

solution, the as-prepared samples were characterized by UV-vis spectroscopy because absorption spectroscopy is a simple experimental tool for investigating surface plasmon resonance (SPR) properties of coinage metal NPs[29]. Fig.3 shows the absorption spectra of AgNPs and Ag@PMBA@C@Au hybrid NPs with different Au to Ag molar ratios. The samples of AgNPs and Ag@PMBA@C NPs exhibit one relative narrow absorption band. For pure AgNPs, the peak is at 417 nm, corresponding to silver SPR (Fig.3(a)). For Ag@PMBA@C NPs, the peak is red-shifted from 417 nm to 428 nm due to the variation of medium dielectric constant induced by C shell (Fig.3(b))[30]. When the AuNPs adsorbed on the Ag@PMBA@C NPs, the absorption band was broadened and further red-shifted to higher wavelengths. In this case, the band consists of three parts: the shorter part corresponding to silver SPR, the longer part corresponding to gold SPR, and the rest coming from the SPR coupling of AgNP and AuNP[31]. Moreover, the larger the molar ratio (Au to Ag) is, the more AuNPs are contained in composite. Thus, the SPR band of Ag decreases and the SPR band of Au increases with the increase of the amount of $HAuCl_4$. When core AgNP is completely covered by AuNPs, the SPR band of AgNP turns to be quite weak and SPR band of AuNP turns to be dominating (Fig.3(e)). These changes in optical properties can be understood as the results of amount variation of the adsorbed AuNPs. It should be pointed out that the treatment of the centrifugation and resuspension is necessary to purify the hybrid NPs.

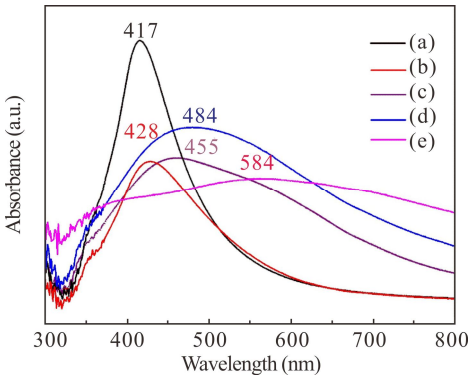


Fig.3 UV-vis absorption spectra of (a) AgNPs and (b-c) Ag@PMBA@C@Au NPs with different Au to Ag molar ratios; The Au to Ag molar ratios are (b) 0: 1.0 (pure Ag@PMBA@C NPs), (c) 0.05: 1.0, (d) 0.15: 1.0, and (e) 0.40: 1.0, respectively

The SERS signals obtained from individual NP are rather weak but SERS signals can be strongly enhanced in the gaps of coinage metal nanostructures due to the coupling of EM field[32,33]. The reporter molecules resided in the gap zone between inner AgNP and outer AuNPs in our prepared core-shell NPs. Therefore, huge Raman signals of the reporter molecules can be obtained and the as-prepared hybrid NPs can be potentially served as SERS labels. In addition, SERS signals can be optimized by adjusting the structure of the hybrid NPs. In the present work, the SERS-active tagging molecules were added and adsorbed on the surface of Ag core at the beginning of preparation of the SERS tagging hybrid NPs. Then the PMBA-modified AgNPs were coated by C shell and AuNPs to form a Ag@PMBA@C@Au bimetallic sandwich structure. This sandwich structure was able to enhance the SERS signals of the tagging molecules remarkably due to the EM coupling between the AgNP and AuNP[34]. Fig.4 shows the SERS spectra of Ag@PMBA@C@Au NPs with different Au to Ag molar ratios. As analyzed above, SERS spectra of the different hybrids display noticeably different intensities. SERS spectra of Ag@PMBA@C@Au NPs are enhanced markedly compared to Ag@PMBA@C. Moreover, with the amount of AuNPs increasing, the intensities of SERS signals of PMBA increase quickly. When the molar ratio of Au to Ag reaches 0.15: 1.0, the SERS signals turn to be the strongest. According to TEM image (Fig.2(c)), the AuNPs have formed a quasi-continuous shell in this case. However, if the amount of Au continues to grow, the intensities of SERS signals will decrease (Fig.4(d)) because over-dense AuNPs block the propagation of light (Fig.2(d)). According to previous literature, two prominent SERS bands of PMBA at 1 586 cm^{-1} and 1 076 cm^{-1} were assigned to the ν_{8a} and ν_{12} aromatic ring vibrations, respectively, and those weak modes at 1 373 cm^{-1} and 841 cm^{-1} were attributed to the ν(COO-) and δ(COO-) vibrations, respectively[35]. The results indicate that hybrid NPs can be utilized as an effective SERS tags with the proper amount of AuNPs due to the excellent SERS-activity.

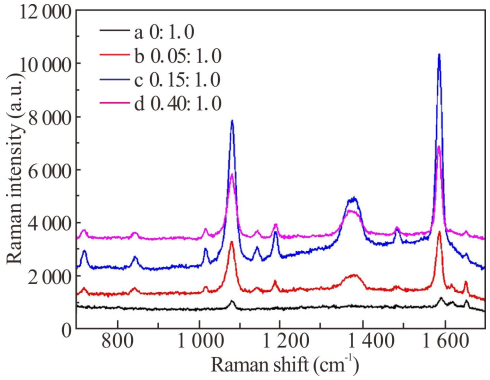


Fig.4 SERS spectra of Ag@PMBA@C@Au NPs with different Au to Ag molar ratios

To clarify the EM enhancement mechanism of Ag@PMBA@C@Au hybrid NPs, three-dimensional finite-difference time domain (FDTD) simulation was performed to investigate the distribution of EM field near the core-shell NPs, which has been widely used to describe EM field of the coinage metal nanostructures. As shown in Fig.5(a), we constructed the model according to the as-prepared samples, which included a

AgNP core with a diameter of 70 nm, a vacuum shell out of AgNP with a thickness of 3 nm, and some AuNPs coated on the shell with a diameter of 5 nm. The excitation source was plane wave with a wavelength at 633 nm. Fig.5(b) shows the distribution of the electric field intensity surrounding the hybrid NPs and between the inner AgNP and outer AuNPs, which gives a maximum $\boldsymbol{E}$-field intensity enhancement $|\boldsymbol{E}/\boldsymbol{E}_0|^2$ over 100. The calculated result indicated that "hot zone" was generated at the gap between the inner AgNP and outer AuNPs due to the coupling of the localized surface plasmon resonance (LSPR) and they were the main contributor of the huge enhancement effect of the composite. On all accounts, based on the theoretical analysis, the SERS signals of the as-prepared labels can be significantly enhanced because the hybrid composite consists of sandwich-structured NPs with a certain nanogap.

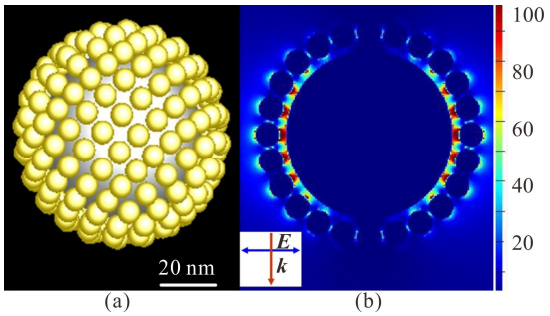


Fig.5 (a) The calculation model and (b) distribution of the simulated electric field intensity of *xy*-plane in which the light is polarized (The *k*- and *E*-vectors indicate the incident direction of laser light and the polarization direction, respectively; The scale bar is 100.)

In conclusion, monodispersed and biocompatible Ag@PMBA@C@Au NP-based SERS labels have been synthesized in a simple method. The hybrid NP is core-multiple shells nanostructure: a AgNP core for SERS enhancement, reporter molecules for SERS signatures, a C shell for protection and isolation, a submonolayer of AuNPs immobilized on top of C layer for further optical enhancement. The morphology of the Ag@PMBA@C@Au NPs could be tuned by adjusting the molar ratio of Au to Ag, which further induces the changes of their optical property. The result of SERS measurement shows that the sandwich structure leads to a great enhancement of the Raman signals of labeling molecules. The as-prepared reporter-embedded hybrid core-shell NP can provide SERS signals of high reproducibility and stability, which is expected to have practical application as an effective SERS label in bioanalytical application.

Ethics declarations

Conflicts of interest

The authors declare no conflict of interest.

References

[1] NIE S M, EMERY S R. Probing single molecules and single nanoparticles by surface-enhanced Raman scattering[J]. Science, 1997, 275(5303): 1102-1106.

[2] SITJAR J, XU H Z, LIU C Y, et al. Synergistic surface-enhanced Raman scattering effect to distinguish live SARS-CoV-2 S pseudovirus[J]. Analytica chimica acta, 2022, 1193: 339406.

[3] YADAV S, KHANAM R, SINGH J P. A purview into highly sensitive magnetic SERS detection of hemozoin biomarker for rapid malaria diagnosis[J]. Sensors and actuators B-chemical, 2022, 355: 131303.

[4] MCDONNELL C, ALBARGHOUTHI F M, SELHORST R, et al. Aerosol jet printed surface-enhanced Raman substrates: application for high-sensitivity detection of perfluoroalkyl substances[J]. ACS omega, 2023, 8(1): 1597-1605.

[5] ZHAO W S, YANG S, ZHANG D X, et al. Based on optimized aptamers-functionalized magnetic capture probes and graphene oxide-Au nanostars SERS tags[J]. Journal of colloid and interface science, 2022, 634: 651-663.

[6] LI P Z, XIA X H, CHEN J N, et al. Morphology-regulated core-shell Ag@Au NPs for rapid SERS detection of 1-amino-hydantoin (AHD) in crayfish[J]. Food and agricultural immunology, 2022, 33(1): 832-847.

[7] ZHAO M M, LIU W Y, DU J G, et al. Multidimensional Co_3O_4 nano sponge for the highly sensitive SERS applications[J]. Optoelectronics letters, 2017, 13(1): 38-41.

[8] DOERING W E, NIE S M. Spectroscopic tags using dye-embedded nanoparticles and surface-enhanced Raman scattering[J]. Analytical chemistry, 2003, 75(22): 6171-6176.

[9] CAO Y W, JIN R C, MIRKIN C A. Nanoparticles with Raman spectroscopic fingerprints for DNA and RNA detection[J]. Science, 2002, 297: 1536-1540.

[10] YAN M M, LI H D, LI M, et al. Advances in surface-enhanced Raman scattering-based aptasensors for food safety detection[J]. Journal of agricultureal and food chemistry, 2021, 69(47): 14049-14064.

[11] SHANMUKH S, JONES L, DRISKELL J, et al. Rapid and sensitive detection of respiratory virus molecular signatures using a silver nanorod array SERS substrate[J]. Nano letters, 2006, 6(11): 2630-2636.

[12] DOERING W E, PIOTTI M E, NATAN M J, et al. SERS as a foundation for nanoscale optically detected biological labels[J]. Advanced materials, 2007, 19: 3100-3108.

[13] WANG C G, CHEN Y, WANG T T, et al. Monodispersed gold nanorod-embedded silica particles as novel Raman labels for biosensing[J]. Advanced functional materials, 2008, 18(2): 55-361.

[14] KONG K V, LAM Z Y, LAU W K O, et al. A transition metal carbonyl probe for use in a highly specific and sensitive SERS-based assay for glucose[J]. Journal of the American chemical society, 2013, 135(48): 18028-18031.

[15] NIE B B, LUO Y Y, SHI J P, et al. Bowl-like pore array made of hollow Au/Ag alloy nanoparticles for SERS detection of melamine in solid milk powder[J]. Sensors and actuators B-chemical, 2019, 301: 127087.

[16] LI S Z, PEDANO M L, CHANG S H, et al. Gap structure effects on surface-enhanced Raman scattering intensities for gold gapped rods[J]. Nano letters, 2010, 10(5): 1722-1727.

[17] YAMAMOTO Y S, ITOH T. Why and how do the shapes of surface-enhanced Raman scattering spectra change? Recent progress from mechanistic studies[J]. Journal of Raman spectroscopy, 2016, 47(1): 78-88.

[18] ITOH T, YOSHIDA K, ISHIKAWA M. Experimental demonstration of the electromagnetic mechanism underlying surface enhanced Raman scattering using single nanoparticle spectroscopy[J]. Journal of photochemistry and photobiology A-chemistry, 2011, 219(2-3): 167-179.

[19] DVOYNENKO M M, WANG J K. Finding electromagnetic and chemical enhancement factors of surface-enhanced Raman scattering[J]. Nano letters, 2007, 32(24): 3552-3554.

[20] SHIN K S. Effect of surface morphology on surface-enhanced Raman scattering of 4-aminobenzenethiol adsorbed on gold substrates[J]. Journal of Raman spectroscopy, 2008, 39(4): 468-473.

[21] KIM J, JANG Y, KIM N J, et al. Study of chemical enhancement mechanism in non-plasmonic surface enhanced Raman spectroscopy (SERS)[J]. Frontiers in chemistry, 2019, 7: 582.

[22] LAN L L, GAO Y M, FAN X, et al. The origin of ultrasensitive SERS sensing beyond plasmonics[J]. Frontiers of physics, 2021, 16(4): 43300.

[23] LI W Y, CAMARGO P H C, LU X M, et al. Dimers of silver nanospheres: facile synthesis and their use as hot spots for surface-enhanced Raman scattering[J]. Nano letters, 2009, 9(1): 485-490.

[24] DADOSH T, SPERLING J, BRYANT G W, et al. Plasmonic control of the shape of the Raman spectrum of a single molecule in a silver nanoparticle dimer[J]. ACS nano, 2009, 3(7): 1988-1994.

[25] SHEN A G, CHEN L F, XIE W, et al. Triplex Au-Ag-C core shell nanoparticles as a novel Raman label[J]. Advanced functional materials, 2010, 20(6): 969-975.

[26] SUN X M, LI Y D. Ag@C core/shell structured nanoparticles: controlled synthesis, characterization, and assembly[J]. Langmuir, 2005, 21: 6019-6024.

[27] ZHANG X J, LU Z Y, SIM D H, et al. Controlled synthesis of Ag/Ag/C hybrid nanostructures and their surface-enhanced Raman scattering properties[J]. Chemistry-A European journal, 2011, 17(48): 13386-13390.

[28] ORENDORFF C J, GOLE A, SAU T K, et al. Surface-enhanced Raman spectroscopy of self-assembled monolayers: sandwich architecture and nanoparticle shape dependence[J]. Analytical chemistry, 2005, 77(10): 3261-3266.

[29] MAYE M M, NYKYPANCHUK D, CUISINIER M, et al. Stepwise surface encoding for high-throughput assembly of nanoclusters[J]. Nature materials, 2009, 8: 388-391.

[30] CAO M, WANG M, GU N. Calculated optical properties of dielectric shell coated gold nanorods[J]. Chinese physics letters, 2009, 26(4): 045201.

[31] PENA-RODRIGUEZ O, PAL U. Enhanced plasmonic behavior of bimetallic (Ag-Au) multilayered spheres[J]. Nanoscale research letters, 2011, 6: 279.

[32] YANG M, ALVAREZ-PUEBLA R, KIM H S, et al. SERS-active gold lace nanoshells with built-in hotspots[J]. Nano letters, 2010, 10(10): 4013-4019.

[33] KLEINMAN S L, RINGE E, VALLEY N, et al. Single-molecule surface-enhanced Raman spectroscopy of crystal violet isotopologues: theory and experiment[J]. Journal of the American chemistry society, 2011, 133(11): 4115-4122.

[34] ZHU C H, MENG G W, HUANG Q, et al. Au hierarchical micro/nanotower arrays and their improved SERS effect by Ag nanoparticle decoration[J]. Crystal growth & design, 2011, 11(3): 748-752.

[35] KAMINSKA A, DZIECIELEWSKI I, WEYHER J L, et al. Highly reproducible, stable and multiply regenerated surface-enhanced Raman scattering substrate for bio-medical applications[J]. Journal of materials chemistry, 2011, 21(24): 8662-8669.